INTERNATIONAL SOCIETY FOR
SOIL MECHANICS AND
GEOTECHNICAL ENGINEERING

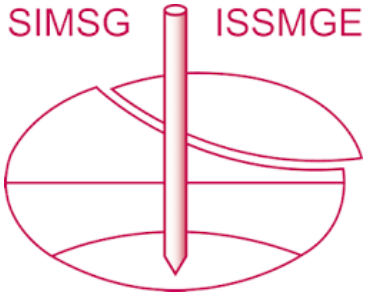

This paper was downloaded from the Online Library of the International Society for Soil Mechanics and Geotechnical Engineering (ISSMGE). The library is available here:

https://www.issmge.org/publications/online-library

This is an open-access database that archives thousands of papers published under the Auspices of the ISSMGE and maintained by the Innovation and Development Committee of ISSMGE.

The paper was published in the proceedings of the 7th International Conference on Earthquake Geotechnical Engineering and was edited by Francesco Silvestri, Nicola Moraci and Susanna Antonielli. The conference was held in Rome, Italy, 17 – 20 June 2019.

Earthquake Geotechnical Engineering for Protection and Development of Environment and Constructions – Silvestri & Moraci (Eds)
© 2019 Associazione Geotecnica Italiana, Rome, Italy, ISBN 978-0-367-14328-2

Numerical simulation of dense sand behavior under multi-directional seismic loading using a new 3-D constitutive model

O.A. Numanoglu, Y.M.A. Hashash & S.M. Olson
University of Illinois at Urbana-Champaign, USA

A. Cerna-Diaz
AECOM, USA

L. Bhaumik
Mott MacDonald, USA

C.J. Rutherford
Iowa State University, USA

T. Weaver
U.S. Nuclear Regulatory Commission, USA

ABSTRACT: Saturated, dense sands subjected to strong shaking from earthquakes may not liquefy but can experience total and differential settlements that can impair an overlying structure. Many available studies and procedures have focused on liquefaction-induced seismic settlements or settlements due to seismic compression in loose to medium-dense sands under uni-directional loading. In contrast, there are few studies related to the shear and volumetric response of dense to very dense saturated sands under multi-directional seismic loading. In this study, a 3-D, distributed element plasticity-based, effective mean stress-dependent constitutive model (I-soil) is introduced for dense to very dense sands. This constitutive model captures: (1) both Masing and non-Masing type hysteretic behavior; (2) small strain nonlinearity; and (3) shear-induced volumetric behavior including settlement and excess porewater pressure generation/dissipation. The model parameters defining shear stress – shear strain behavior are determined using shear wave velocity, a normalized strain-dependent modulus reduction curve, and damping curve. Shear induced volumetric response is calibrated using shear strain – volumetric strain response data from laboratory tests. The resulting model was implemented in a dynamic finite element analysis program and can capture the shear and volumetric behavior of saturated sands (with relative densities of 65 to 100%) measured in cyclically loaded laboratory specimens, as well as free-field and soil-structure system dynamic centrifuge tests. The simplicity of the mathematical formulation of the constitutive model allows the simulation of full scale 3-D soil-structure interaction problems within a couple of hours using single and multi-CPU simulations on a personal computer.

1 INTRODUCTION

Nuclear power plants (NPPs) constructed on compacted, dense sand deposits may experience non-trivial settlements if the deposit is thick enough. For example, Silver and Seed (1969) showed that a clean, dry sand specimen with a relative density (D_R) of 80% can experience vertical strains (ε_v) of 0.3% at the end of 10 cycles of uniform shearing with cyclic shear strain (γ_c) amplitude of 0.5%. For a 20 m thick clean sand deposit, ε_v = 0.3% results in 6 cm of settlement –enough to impair the foundation of an NPP. The Kashiwazaki-Kariwa Nuclear Power Station experienced fire damage following the 2007 Niigata-kend Chuetsu-oki earthquake as a result of seismic settlement of a transformer foundation supporting non-safety related equipment. The earthquake

induced an average vertical strain of 0.8% and 20 cm of settlement in a 25-m-thick saturated coarse-grained backfill (D_R = 60-100%). The settlement resulted in pipe breaks and oil leaks that caused the fire (Sakai et al. 2009). Yee et al. (2011) also showed that Service Hall Building at Kashiwazaki-Kariwa NPP site settled 10 to 20 cm (average $\varepsilon_v \sim 0.2\%$). This building was founded on a 70-m-thick profile of medium dense to dense sand (ground water table was 45 m below the ground surface) overlying clayey bedrock. Similarly, the main control building of the Jensen Filtration Plant settled 12 – 15 cm due to an average vertical strain of 0.8% in a medium-dense, clayey sand fill during the 1971 San Fernando earthquake. This settlement resulted in extensive structural damage (Pyke et al. 1975). These studies demonstrate the significance of seismic settlements of dense sands, regardless of saturation.

Over the past 60 years many studies have addressed the volumetric response of sand during earthquake loading. These studies are mainly separated into: (1) simplified semi-empirical procedures; and (2) advanced numerical modeling and simulations. Semi-empirical procedures are widely used in both research and practice and provide first-order estimates of seismic settlements. Several semi-empirical methods provide separate estimation of seismic settlements for drained and undrained conditions [e.g., Silver and Seed (1969), Tokimatsu and Seed (1984), Ishihara and Yoshimine (1992)]. More recent studies conducted by Bray and Macedo (2017) and Bullock et al. (2018) provide semi-empirical correlations for estimating liquefaction-induced settlements. Furthermore, Elgamal et al. (2002), Dafalias and Manzari (2004) and Boulanger and Ziotopoulou (2012) have proposed constitutive models to estimate the dynamic response of clean sands. These methods have been used extensively in boundary value problems to estimate seismic settlements and/or excess porewater pressure response of free-field and soil-structure systems [e.g., Karimi and Dashti (2016), Bullock et al. (2018), Ramirez et al. (2018), Ziotopoulou (2018), Ghofrani and Arduino (2018)]. Most of the available studies have focused on the uni-directional seismic response of liquefiable systems and geometrically simplified boundary value problems (i.e., 2-D or partial geometry that considers symmetry). Han et al. (2017) utilized the Imperial College Generalized Small Strain Stiffness (ICG3S) model to estimate multi-directional seismic response of a KiK-net downhole array. They found that different calibrations were required for different earthquake magnitudes.

This paper introduces a 3-D constitutive model, designated I-soil, that captures small-strain nonlinearity, hysteretic damping, and shear-induced volumetric response of sands in effective stress space. Small-strain nonlinearity is represented by piecewise nonlinear stress-strain behavior. Hysteretic damping is represented by the generalized hysteretic damping formulation proposed in Numanoglu et al. (2017) which allows both Masing and non-Masing type un/reloading rules. And, the shear-induced volumetric response is captured using a non-associative flow rule.

2 MODEL FORMULATION

The one dimensional framework of I-soil is represented by parallel distributed spring-slider nested components as proposed by Iwan (1967), and can be expressed as:

$$\tau(\gamma) = \sum_{i=1}^{m} \tau_{iy} + \sum_{i=m+1}^{n} G_i \gamma \tag{1}$$

where the summation from i = 1 to m includes all the nested components that have yielded, and the summation from i = m+1 to n includes all the nested components that remain elastic after loading to a shear strain of γ. In other words, equation (1) is a simple formulation to model piece-nonlinear behavior in a piecewise linear fashion by summing the tangent stiffnesses of nested components at a given shear strain. This process can be summarized as follows.

1. Each nested component in the model is subjected to the same total shear strain as experienced by the parallel-series system itself.

2. Each component responds to the applied shear strain in an ideal elasto-plastic way. This provides the characteristics of invariant yield surfaces for 3-D extension.
3. All the components have different stiffness and yield strength. However, the yield criteria have the same form for each component.
4. The model stress is computed by summing the component stresses.

Three-dimensional extension of the model closely follows the generalization proposed by Chiang and Beck (1994) and incorporates formulations for shear-induced volumetric response and non-Masing un/reloading behavior. The stresses in tensorial notation are written as:

$$\dot{\boldsymbol{\sigma}}_{\mathrm{ij}} = \sum_{\mathrm{c}=1}^{\mathrm{n}} \underline{\sigma}_{\mathrm{ij}}^{\mathrm{c}} \tag{2}$$

where $\dot{\sigma}_{ij}$ is the second-order Cauchy effective stress rate tensor for the model stresses whereas $\dot{\sigma}^{c}_{ij}$ is the same quantity in component stress space with superscript "c" indicating the component number. Drucker-Prager type conical yield surfaces are used to define plastic loading and the yield function takes following form:

$$f^{c} = \left(\frac{1}{2} s^{c}_{ij} s^{c}_{ji}\right)^{0.5} - \left(\frac{a_0 + a_1\left[\frac{\sigma_{kk}}{3} - \sigma'_0\right] + a_2\left[\frac{\sigma_{kk}}{3} - \sigma'_0\right]^2}{a_0 + a_1\left(\sigma'_{ref}\right) + a_2\left(\sigma'_{ref}\right)^2}\right)^{0.5} \tau^{c}_{y} \tag{3}$$

where a_0, a_1 and a_2 are flags to determine effective mean stress dependency of the yield function (e.g., $a_0 = 0$, $a_1 = 0$, $a_2 = 1$ leads to linear dependency), σ'_{ref} is the reference effective mean stress at which the mean stress dependent parameters are initially defined, σ'_0 is a small negative (tensile) effective mean stress below which the $\sigma_{kk}/3$ term in equation (3) is set to zero, and $s_{ij} = \sigma_{ij} - (\sigma_{kk}/3)\delta_{ij}$ is the deviatoric stress tensor, and τ^{c}_{y} is the initial yield strength of the nested component. Plastic deviatoric strains are calculated using an associative flow rule whereas the plastic volumetric strains are computed by non-associative flow rules as:

$$\dot{\varepsilon}^{\mathrm{c}}_{\mathrm{ii}} = \mathrm{A}_0(\eta_{\mathrm{pt}} - \eta)\dot{\gamma} \tag{4}$$

where $\underline{\varepsilon}^{c}_{ii}$ is the tensorial representation of the volumetric strain rate, γ is the rate of the second invariant of the deviatoric strain tensor, η is the shear stress ratio, η_{pt} is the dilatancy stress ratio [commonly referred as phase transformation stress ratio (Ishihara et al. 1975)], and A_0 is a model parameters that controls the magnitude of the rate of shear-induced volumetric strain. The form used in (4) was first proposed by Nova and Wood (1979) based on Rowe (1962). The hysteretic response is modeled using the Numanoglu et al. (2017) formulation.

I-soil model was implemented in LS-DYNA (LSTC 2009) and MASTODON (Coleman et al. 2018). The model inputs are: (1) $G/G_{max} - \gamma$ curve, Poisson's ratio, and hysteretic damping parameters (p_1, p_2, and p_3, as proposed by Phillips and Hashash (2009). Numanoglu (in progress) presents a detailed derivation of the I-soil model. Model calibration and application for multi-directional boundary value problems within LS-DYNA are discussed in next sectionss.

3 COMPARISON TO CYCLIC DIRECT SIMPLE SHEAR TEST

This section illustrates the performance of I-soil using a K_0-consolidated constant volume cyclic direct simple shear test (K_0cDSS) conducted by Sibley (2016). The reconstituted specimen consisted of a fine-grained sand (Salt Fork River sand) at D_R = 65% and a consolidation vertical stress = 100 kPa. Empirical normalized modulus reduction and damping curves from Darendeli (2001) together with the shear wave velocity correlation proposed by Menq (2003) were used to develop the input backbone curve for I-soil, and the shear strength correction in the GQ/H model (Groholski et al. 2016) was used to better represent mobilized large-strain shear strength (for $\phi' = 34°$). Figure 1 shows the normalized modulus reduction, damping and shear stress –

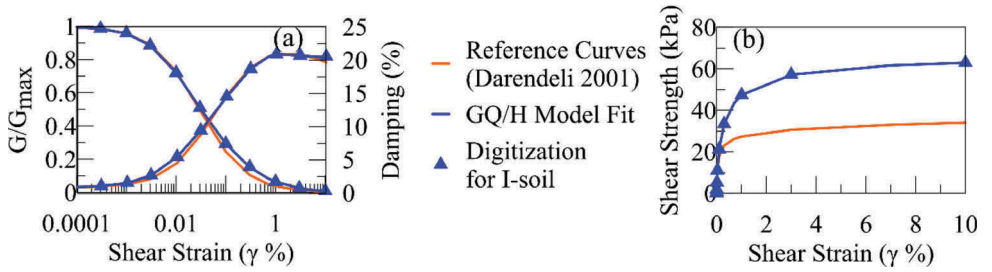

Figure 1. Selectedparameters for I-soil model for element test simulations. (a) Normalized modulus reduction and damping; and (b) shear stress – shear strain curves.

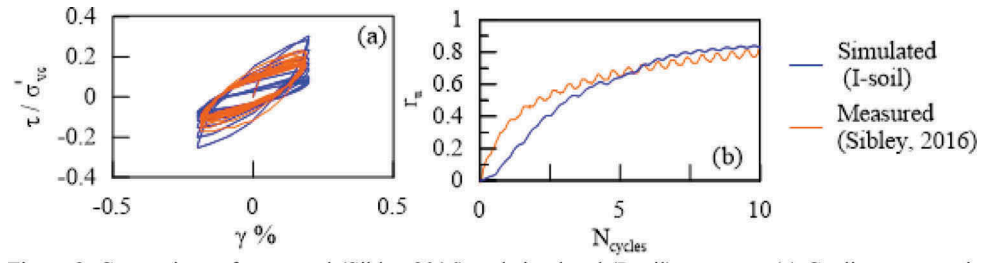

Figure 2. Comparison of measured (Sibley 2016) and simulated (I-soil) response. (a) Cyclic stress-strain; and (b) excess pore-water pressure response for medium-dense (D_R = 65%) Salt Fork River sand specimen consolidate to effective vertical stress of 100 kPa.

shear strain curves used for I-soil. Numanoglu (in progress) compiled 51 laboratory tests including undrained and drained triaxial compression and extension, drained DSS and cyclic hollow cylinder torsional shear tests, and computed an average dilatancy stress ratio of 0.55 for variety of sand specimens having different relative densities and confining pressures. Finally, the fitting parameter A_0 = 0.15 was determined by trial-and-error using several sand specimens including Ottawa C109, Salt Fork River, Sangamon River and Nevada sands until good agreement was achieved between the measured and computed response for single element tests in terms of shear induced excess porewater pressure due to contractive/dilative tendency.

Figure 2 compares representative results for measurements presented in Sibley (2016) and simulation obtained from single element test. Figure 2a present measured and simulated cyclic shear stress – shear strain response for γ_c = 0.2% applied on medium-dense Salt Fork River sand. Initially, the estimated response was observed to be slightly stiffer than the measured counterpart. Therefore, initially, the rate of excess porewater pressure generation is slower (Figure 2b). However, at later cycles both simulations and measurements agree well in terms of hysteretic behavior and cyclic degradation due to excess porewater pressure generation, reaching a maximum $r_u \sim 0.8$. After 10 cycles, the simulation exhibited slightly higher degradation.

4 APPLICATION TO MULTI-DIRECTIONAL SITE RESPONSE AND SSI ANALYSES

I-soil model response also was compared to multi-directional free-field dynamic centrifuge test results. The centrifuge tests were conducted at Rensselaer Polytechnic Institute and presented by Cerna Diaz (2018) and Cerna-Diaz et al. (2017). The centrifuge soil profile (prototype scale) consisted of a saturated, very dense (D_R = 95%), 22-m thick deposit of Ottawa 40/70 sand, which has a median particle size, D_{50} = 0.28 mm and a uniformity coefficient, C_u = 1.36. Olson et al. (2015), Bhaumik et al. (2017), and Cerna-Diaz et al. (2017) provide additional details. The

same procedure as described above was used to construct the I-soil backbone curve, with the parameters modeling shear induced volumetric response remaining the same as they were in element level simulation. The only exception was that depth-dependent profiles of friction angle and shear wave velocity (V_s) were defined using correlations from Bolton (1986) and Menq (2003), respectively. The Menq (2003) correlation closely matched bender element V_s values measured in the centrifuge. Figure 3 shows the depth-dependent properties. Small-strain damping was represented using a frequency-independent damping formulation implemented in LS-DYNA. For the shear beam analysis, the finite element model was meshed in accordance with the $V_s/4H > 30$ Hz recommendation (Hashash et al. 2010), where H is layer thickness.

The bottom boundary of the shear beam model was modeled as a rigid base with prescribed accelerations corresponding to Landers (1992) earthquake recorded at 20.5 m depth of the centrifuge model. The ground water table was defined at the surface and simulations were run in a partially drained condition with permeability of $5x10^{-4}$ m/sec estimated from Hazen's equation.

Figure 4 compares the computed and measured spectral response, settlements and excess porewater pressures at a depth of 2 m. The comparison shows that the peak accelerations and spectral accelerations between 0.01 sec and 0.15 sec are overestimated by 50%, while good agreement was observed at periods larger than 0.15 sec. The discrepancy at higher frequencies

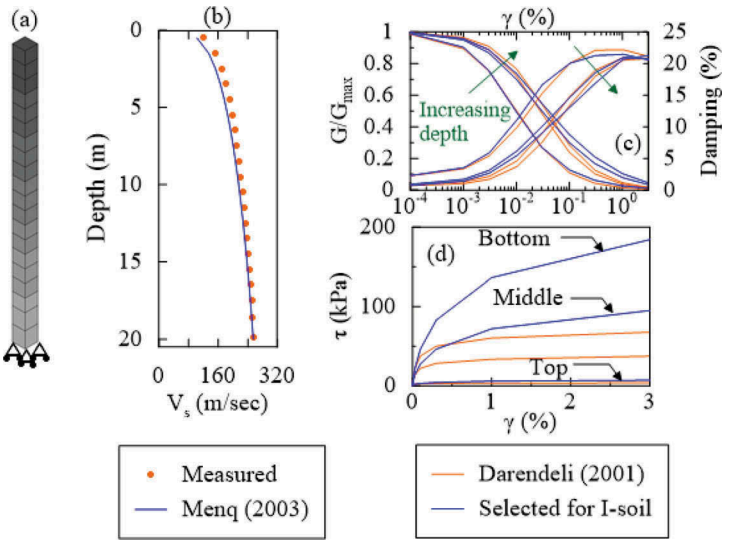

Figure 3. Input profile for multi-directional computational analysis. (a) Finite element discretization; (b) V_s profile; (c) modulus reduction and damping curves; and (d) backbone curves.

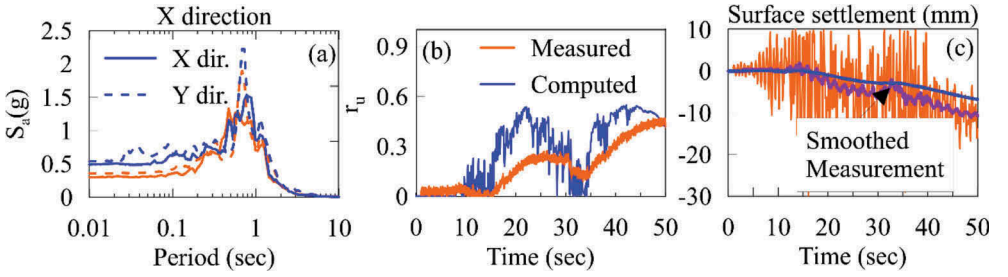

Figure 4. Comparison of measured and computed multi-directional site response results for Ottawa sand (D_R = 95%) dynamic centrifuge test. (a) 5% damped spectral response for x- and y-directions; (b) shaking-induced excess porewater pressure; and (c) shaking-induced settlements.

may be due to larger dilation spikes computed in simulations which may lead to higher instantaneous stiffness gain. However, further research is needed to quantify the effect of dilative tendency on spectral response.

The trends and maximum settlements and excess porewater pressures during shaking were captured reasonably well with approximately 10 mm of settlement and a maximum $r_u \sim 0.5$. The numerical I-soil model was able to capture qualitatively the combination of excess porewater pressure generation, dissipation and drops due to dilative spikes.

The same input parameters and curves that were utilized in the multi-directional site response simulations were used to simulate a SSI system with bi-directional shaking. Figure 5a shows the centrifuge test model before the final fill was placed to embed the structure, the meshed geometry for the finite element model, and locations of instruments selected for comparison. The centrifuge sand model was saturated, therefore a zero porewater pressure boundary was defined at the surface in the numerical model. Steel rings of the centrifuge container were approximated as a periodic boundary condition at the nodes (at the same elevation as the rings) on the exterior boundaries. This boundary condition dictates equal displacements in each direction for the nodes at the same elevation at the exterior sides of the soil domain. The structure was modeled as a rigid material, and the soil-structure interface was defined as an impermeable boundary.

Figures 5b, c, and d compare the computed and measured spectral accelerations under the structure,structure settlement, and excess porewater pressures under the structure, respectively. As illustrated in the figure, measured and computed settlements agreed reasonably, both indicating ~10 mm of structure settlement. Peak ground accelerations and spectral responses in each direction were captured reasonably, with only ~25% underestimation in y-direction response near a period of ~0.8 sec and 100% overestimation at period of ~0.5 sec. The trends of excess porewater pressure generation, dissipation, and dilative response were captured, although the numerical model significantly overestimated the measured variations. However, this overestimation was considered to be insignificant since the r_u below the structure was very low (r_u<0.05). Simulation run times (total CPU hours) for a 70-second base motion using 1 and 4 cores were 9 hours, 39 minutes and 3 hours, 29 minutes, respectively.

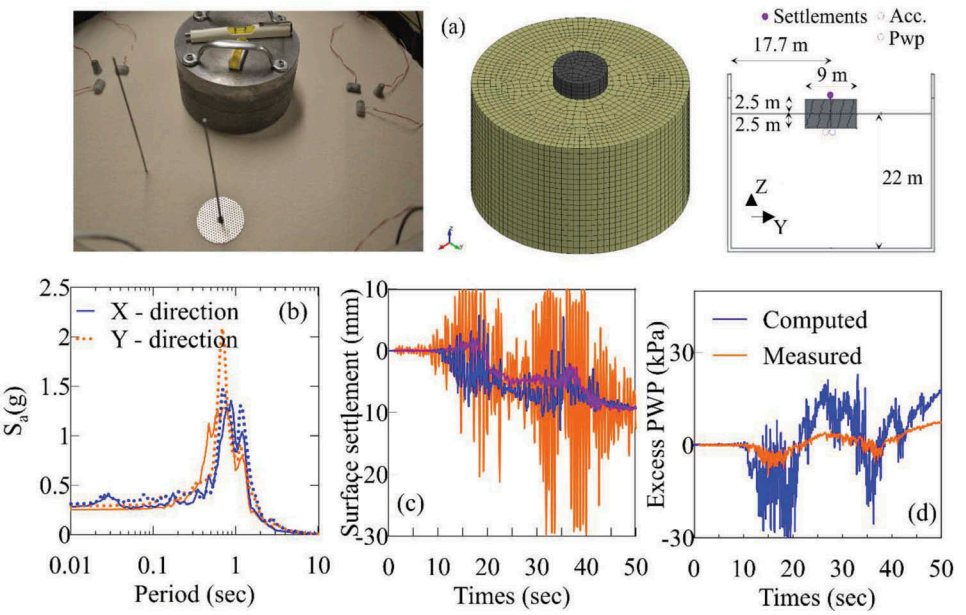

Figure 5. SSI numerical simulation details and comparison to measured data for seismic soil-fluid-structure interaction for D_R = 95% Ottawa sand centrifuge model. (a) Centrifuge specimen, numerical discretization and location of compared instruments; (b) spectral response; (c) settlement time history; and (d) excess pore-water pressure time history.

5 CONCLUSION

This paper introduces a new 3-D constitutive model, termed I-soil that can be used to represent small-strain nonlinearity, hysteretic damping, and shear-induced volumetric response for medium-dense to very dense sands. The model needs only two parameters in addition to the inputs incorporated in a conventional 1-D nonlinear site response analysis. A consistent parameter definition and calibration were applied for the constitutive model to simulate element level and large-scale experiments. Shear stress – shear strain response utilizes shear wave velocity,strain-dependent normalized modulus reduction and damping curves, and cyclic direct simple shear test results. The laboratory test data was used to calibrate non-associated flow rule parameter that controls the magnitude of shear-induced volumetric response. The simulations described in the paper demonstrated that the constitutive model implemented in a finite element analysis framework is capable of computing shear and volumetric response of clean sands with relative densities of 65-100%, as measured in constant volume cyclic direct simple shear tests as well as partially drained free-field and soil-structure interaction multi-directional dynamic centrifuge experiments. Run times for large-scale models were less than 10 hours and 4 hours, respectively, for single and multi-core simulations. Validation of the proposed I-soil model using a suite of ground motions as well as more experimental and field data under variety of saturation and loading conditions is underway.

ACKNOWLEDGEMENTS

Support for this work was provided by the US Nuclear Regulatory Commission under award number NRC-HQ-12-C-04-0117. Any opinions, findings, and conclusions or recommendations expressed in this document are those of the authors and do not necessarily reflect those of the USNRC

REFERENCES

Bhaumik, L., C. J.Rutherford, A.Cerna-Diaz, S. M.Olson, O. A.Numanoglu, Y. M. A.Hashash and T. Weaver (2017). Volumetric strain in non-plastic silty sand subjected to multidirectional cyclic loading. Geofrontiers 2017: 150-159.

Bolton, M. D. (1986). "The Strength and Dilatancy of Sands." Geotechnique **36**(1): 65-78.

Boulanger, R. W. and K.Ziotopoulou (2012). PM4Sand (Version 2): A Sand Plasticity Model for Earthquake Engineering Applications. Department of Civil and Environmental Engineering, University of California at Davis.

Bray, J. D. and J.Macedo (2017). "6th Ishihara lecture: Simplified procedure for estimating liquefaction-induced building settlement." Soil Dynamics and Earthquake Engineering **102**: 215-231.

Bullock, Z., Z.Karimi, S.Dashti, K.Porter, A. B.Liel and K. W.Franke (2018). "A Physics-informed semi-empirical probabilistic model for the settlement of shallow-founder structures on liquefiable soils." Geotechnique: 1-34.

Cerna-Diaz, A., S. M.Olson, O. A.Numanoglu, Y. M. A.Hashash, C. J.Rutherford, L.Bhaumik and T. Weaver (2017). Free-field cyclic response of dense sands in dynamic centrifuge tests. Geotechnical Frontiers *2017*: 121-130.

Cerna Diaz, A. A. (2018). Evaluation of cyclic behavior of dense sands under multidirectional loading using centrifuge tests. PhD, University of Illinois at Urbana-Champaign.

Chiang, D. Y. and J. L.Beck (1994). "A new class of distributed-element models for cyclic plasticity—I. Theory and application." International journal of solids and structures **31**(4): 469-484.

Dafalias, Y. F. and M. T.Manzari (2004). "Simple plasticity sand model accounting for fabric change effects". Journal of Engineering Mechanics **130**(Special Issue: Constitutive Modeling of Geomaterials).

Darendeli, M. B. (2001). Development of a new family of normalized modulus reduction and material damping curves Ph. D., University of Texas at Austin.

Elgamal, A., Z. H.Yang and E.Parra (2002). "Computational modeling of cyclic mobility and post-liquefaction site response." Soil Dynamics and Earthquake Engineering **22**(4): 259-271.

Ghofrani, A. and P.Arduino (2018). "Prediction of LEAP centrifuge test results using a pressure-dependent bounding surface constitutive model." Soil Dynamics and Earthquake Engineering **113**: 758-770.

Groholski, D. R., Y. M. A.Hashash, B.Kim, M.Musgrove, J.Harmon and J. P.Stewart (2016). "Simplified Model for Small-Strain Nonlinearity and Strength in 1D Seismic Site Response Analysis." Journal of Geotechnical and Geoenvironmental Engineering **142**(9): 04016042.

Han, B., L.Zdravkovic, L.Kontoe and D. M.Taborda (2017). "Numerical investigation of multi-directional site response based on KiK-net downhole array monitoring data." Computers and Geotechnics **89**: 55-70.

Hashash, Y. M. A., C.Phillips and D. R.Groholski (2010). Recent advances in non-linear site response analysis. Fifth International Conference in Recent Advances in Geotechnical Eartqhuake Engineering and Soil Dynamics. San Diego, CA. **CD-Volume**: OSP 4.

Ishihara, K., F.Tatsuoka and S.Yasuda (1975). "Undrained deformation and liquefaction of sand under cyclic stresses." Soils and Foundations **15**(1): 29-44.

Ishihara, K. and M.Yoshimine (1992). "Evaluation of settlements in sand deposits following liquefaction during earthquakes." Soils and Foundations **32**(1): 173-188.

Iwan, W. D. (1967). "On a class of models for the yielding behavior of continuous and composite systems." Jour. Apl. Mech., Trans. ASME **34**(E3): 612-617.

Karimi, Z. and S.Dashti (2016). "Numerical and Centrifuge Modeling of Seismic Soil-Foundation-Structure Interaction on Liquefiable Ground." Journal of Geotechnical and Geoenvironmental Engineering **142**(1).

Menq, F. Y. (2003). Dynamic Properties of Sandy and Gravelly Soils Ph.D, University of Texas at Austin.

Nova, R. and D. M.Wood (1979). "A constitutive model for sand in triaxial compression." International Journal for Numerical And Analytical Methods in Geomechanics **3**(3): 255-278.

Numanoglu, O. A. (in progress). Numerical Modeling and Simulation of Seismic Settlements in Dense Sands under Multi-directional Loading. PhD, University of Illinois at Urbana-Champaign.

Numanoglu, O. A., M. M.Musgrove, J. A.Harmon; and Y. M. A.Hashash (2017). "Generalized non-Masing hysteresis model for cyclic loading." Journal of Geotechincal and Geoenvironmental Engineering **144**(1): 06017015.

Olson, S. M., Y. M. A. R. Hashash, C.J., A. N. Cerna-Diaz, O.A. and B. L.A. (2015). Experimental and numerical investigation of cyclic response of dense sand under multidirectional shaking. Proc. of 6th International Conference on Earthquake Geotechnical Engineering

Phillips, C. and Y. M. A.Hashash (2009). "Damping formulation for non-linear 1D site response analyses." Soil Dynamics and Earthquake Engineering **29**(7): Pages 1143-1158.

Pyke, R. M., C. K.Chan and H. B.Seed (1975). "Settlement of sands under multidirectional shaking." Journal of the Geotechnical Engineering Division **101**(4): 379-398.

Ramirez, J., A. R.Barrero, L.Chen, S.Dashti, A.Ghofrani, M.Teibat and P.Arduino (2018). "Site response in a layered liquefiable deposit: evaluation of different numerical tools and methodologies with centrifuge experimental results." Journal of Geotechincal and Geoenvironmental Engineering **144**(10).

Rowe, P. W. (1962). "The Stress-Dilatancy Relation for Static Equilibrium of an Assembly of Particles in Contact." Proceedings of the Royal Society of London. Series A, Mathematical and Physical Science **269**(1339): 500-527.

Sakai, T., T.Suehiro and T.Tani (2009). "Geotechnical performance of the Kashiwazaki-Kariwa Nuclear Power Station caused by the 2007 Niigataken Chuetsu-oki earthquake." Case Histoyr Volume for Performance-Based Design in Earthquake Geotechnical Engineering, Technical Committee(4): 1-29.

Sibley, E. (2016). Drained cyclic preshearing effects on the liquefaction resistance of sands. PhD, University of Illinois at Urbana-Champaign.

Silver, M. L. and H. B.Seed (1969). "Volume changes in sands during cyclic loading." Journal of Soil Mechanics and Foundation Division **97**(9): 1171-1182.

Tokimatsu, K. and H. B.Seed (1984). Simplified procedures for the evaluation of settlements in clean sands. Berkely, California, Eathquake Engineering Research Center.

Yee, E., J. P.Stewart and K.Tokimatsu (2011). Nonlinear site response and seismic compression at vertical array strongly shaken by 2007 Niigata-ken Chuetsu-oki earthquake, Pacific Earthquake Engineering Research Center, University of California, Berkeley.

Ziotopoulou, K. (2018). "Seismic response of liquefiable sloping ground: Class A and C numerical predictions of centrifuge model responses." Soil Dynamics and Earthquake Engineering **113**: 744-757